Inorganic Chemistry

Article

pubs.acs.org/IC

Is Octavalent Pu(VIII) Possible? Mapping the Plutonium Oxyfluoride Series PuO_nF_{8-2n} (n = 0−4)

Wei Huang,[†] Pekka Pyykkö,*[,‡] and Jun Li*[,†]

[†]Department of Chemistry and Key Laboratory of Organic Optoelectronics and Molecular Engineering of Ministry of Education, Tsinghua University, 100084 Beijing, People's Republic of China

[‡]Department of Chemistry, University of Helsinki, POB 55, A. I. Virtasen aukio 1, 00014 Helsinki, Finland

Supporting Information

ABSTRACT: While the oxidation state Pu(VIII) is shown to be less stable than Pu(V) in the PuO_4 molecule, it is not clear if the more electronegative fluorine can help to stabilize Pu(VIII). Our calculations on PuO_nF_{8-2n} (n = 0−4) molecules notably confirm that PuO_2F_4 has both $^1D_{4h}$ and $^5C_{2v}$ minima with the oxidation states Pu(VIII) and Pu(V), respectively, with the latter having lower energy. The hybrid-DFT, CCSD(T), and CASSCF methods all give the same result. The results conform to a superoxide ligand when $n \geq 2$. PuF_8 in a ^1O_h state can decompose to PuF_6 and F_2, and $PuOF_6$ in a $^1C_{2v}$ state also can break down to PuF_6 and 1/2 O_2. The Pu(VIII) anion $PuO_2F_5^-$ does have a D_{5h} minimum, which also lies above a $^5C_{2v}$ Pu(V) peroxide structure. However, the energy differences between the different minima are not large, indicating that metastable species with oxidation states higher than Pu(V) cannot be completely excluded.

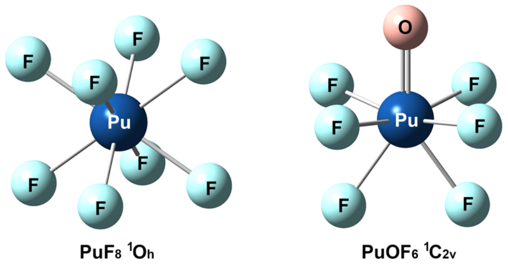

1. INTRODUCTION

The oxidation state is a central concept in chemistry.[1] Early actinides (An) tend to have higher oxidation states (e.g., Th(IV), Pa(V), U(VI), and Np(VII)), while the later actinides prefer the III oxidation state, similar to the case for lanthanides (Ln(III)). Plutonium often lies at the borderline. If all valence electrons of plutonium were formally oxidized away, an f^0d^0 situation analogous to Th(IV) to Np(VII), one would obtain the oxidation state Pu(VIII). While a plethora of lower oxidation states are already known for Pu, the situation concerning octavalent plutonium is still unclear.[2−11] It is moreover interesting to juxtapose this case with that of group 8 transition metals. Among them, the tetrahedral OsO_4 is a commodity chemical, and RuO_4 is also well-known.[12] Considering high oxidation states as such, the situation has been reviewed by Riedel and co-workers.[13,14] As a gas-phase cation or Mössbauer species, $[IrO_4]^+$ is identified to be stable.[14−17] For the heavier noble gases, XeO_4 is known.[12] Our recent work found that achieving a high oxidation state such as VI is rather difficult for later actinides, lanthanides, the seventh-row superheavy elements (e.g., Sg), and the first-row transition metals (e.g., Cr).[18−21] Natural choices for the ligands to achieve high oxidation states of the metals are the highly electronegative fluorine and oxygen.[3]

Returning to actinides, for plutonium and only one type of anion, PuF_8[3] and PuO_4[3,6] are the resulting octavalent compounds. While the volatile PuF_6 is a well-known actinide hexafluoride, used in nuclear technology during the isotope enrichment process,[22−25] the octafluoride PuF_8 is not experimentally well documented. The theoretical literature comprises Straka et al.,[3] who found a cubic O_h structure. Concerning the oxygen ligands, PuO_4 was predicted to be D_{4h},[3] a result verified by ref 11. There are experimental claims based on thermochromatography[26] and on ozonization of Pu(VI) alkaline solutions,[27] combined with radioactivity transfer or optical spectra. They also refer to some earlier work. A possibility that should not be overlooked is that, instead of Pu(VIII) in PuO_4 (D_{4h}), the system may prefer a lower-energy Pu(V) state with one superoxide bound to a slightly bent plutonyl group (see the independent papers by Huang et al.[9] and Zaitsevskii et al.[10,11,28]). Note that actinyl peroxides are a well-known, large class of compounds.[29,30] One might add that the energy difference between PuO_4 and the Pu(V) peroxide is much smaller than that between cyanate (OCN^-) and fulminate (ONC^-), both of which are experimentally known.[31,32] At the preliminary HF/6-31g* level in ref 31 fulminate was estimated to lie 3.3 eV above cyanate. Moreover, the effects of high pressures or special crystal sites have not been studied. Anyway, the challenge of finding and characterizing a lowest-energy, isolated Pu(VIII) molecule remains.

The situation for the mixed oxide-fluoride species $Pu^{VIII}O_nF_{8-2n}$ is so far not conclusive; they might be better or worse as Pu(VIII) candidates. Note that F has a higher electronegativity than O, while O could help to reduce the volume effect. Recall also the inverse trans effect.[33]

A theoretical extreme on the formally high oxidation states of uranium would be the octahedral local minimum of UO_6,[34] which, however, has much lower-lying peroxide isomers.[35] Finally, the calculated atomic ionization potentials of the

Received: July 10, 2015
Published: August 26, 2015

DOI: 10.1021/acs.inorgchem.5b01540
Inorg. Chem. 2015, 54, 8825−8831

superheavy elements suggest that very high oxidation states, such as XII for (E146), could occur for some of them.[36]

Briefly, the purpose of this paper is to take a more tolerant and realistic stand, concerning the possible existence of several energy minima for highly oxidized actinide systems.

2. METHODOLOGY

The calculations were performed with the computational chemical software Gaussian 09,[37] ADF 2013,[38] and MOLPRO 2012[39] using both density functional theory (DFT) and wavefunction theory (WFT). The Supporting Information gives the full citations for the software. In searching for the ground state, a hybrid-DFT B3LYP[40] method was used to optimize the geometry and electronic structure with the Gaussian 09 code. Considering the strong relativistic effects on Pu, we chose an ECP60MWB pseudopotential,[41−43] developed by the Stuttgart−Cologne groups, to include them. We selected the ECP60MWB ANO basis set[42,43] for Pu and the aug-cc-pVTZ basis[44] for O and F. Vibrational frequencies were determined to check the minimum character of all structures.

In order to get more accurate single-point energies of the stationary states, the ab initio single-reference WFT method CCSD(T) (coupled-cluster expansion with single, double, and perturbative triple substitutions)[45−48] was applied with MOLPRO 2012 with the same RECP and basis sets as used in Gaussian 09 calculations. We also employed the multiconfigurational CASSCF method[49] to prove that the systems do not have too large multireference effects, which would make the CCSD(T) energy values unreliable. CASSCF/CASPT2/SO (complete active space self-consistent field/complete active space second-order perturbation theory/spin−orbit coupling)[50,51] was applied to evaluate the spin−orbit effect during PuF_8 decomposition.[52] In this state-interacting (SI) approach, the spin−orbit matrix elements were calculated using spin−orbit pseudopotentials (ECPs) and the CASSCF wave functions. The SO splittings of the electronic states were calculated by diagonalizing the spin−orbit Hamiltonian matrix with the diagonal elements replaced by energies calculated using scalar relativistic CASPT2 methods.

Further analyses of the results were performed with ADF 2013 on the B3LYP level, including transition-state calculations, electronic structure analysis, and bonding analysis. The zero-order regular approximation (ZORA)[53,54] was used to take into account the relativistic effects. All of the atoms use a TZ2P Slater basis set,[55] and the frozen core approximation[56] was applied to the Pu [$1s^2$–$4f^{14}$] core.

3. RESULTS AND DISCUSSION

3.1. Ground States of PuO_nF_{8-2n} (n = 0−4) Species. We present both the ground state of PuO_nF_{8-2n} and the locally stable state with the VIII oxidation state here, except for PuF_8 and $PuOF_6$, where the ground state has an VIII oxidation state. Among the presented states, A−C, E, and G are VIII states and D, F, and H are V states. The calculated B3LYP bond lengths are shown in Table 1, and the structures of the species A−H are shown in Figure 1. The O−O distances are close to the experimental bond length of 1.34 Å for O_2^-.[57] The short Pu−O distances are typical for a triple bond. Similarly, the Pu−F length of slightly over 2 Å is typical for An−F bonds, which actually have some multiple-bond character (see Figure 2 of ref 58).

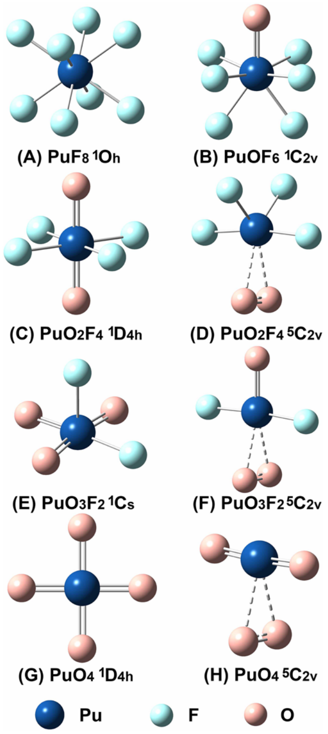

Figure 1. Calculated B3LYP structures of the species A−H.

Table 1. Calculated B3LYP Bond Lengths

		bond length/Å		
species	system	R(Pu−F)	R(Pu−O)	R(O−O)
A	PuF_8 $^1A_{1g}$ (O_h)	2.01		
B	$PuOF_6$ $^1A_1$ (C_{2v})	2.00	1.74	
C	PuO_2F_4 $^1A_{1g}$ (D_{4h})	2.02	1.73	
D	PuO_2F_4 $^5B_1$ (C_{2v})	2.01	2.31	1.32
E	PuO_3F_2 $^1A'$ (C_s)	2.03	1.75	
F	PuO_3F_2 $^5B_1$ (C_{2v})	2.07	1.79, 2.29	1.30
G	PuO_4 $^1A_{1g}$ (D_{4h})		1.77	
H	PuO_4 $^5B_1$ (C_{2v})		1.76, 2.33	1.31

We consider the formation reaction

$$\mathrm{Pu} + 2\mathrm{O}_2 + 4\mathrm{F}_2 \xrightarrow{\Delta_f E} \mathrm{PuO}_n\mathrm{F}_{8-2n} + (2 - n/2)\mathrm{O}_2 + n\mathrm{F}_2 \quad (1)$$

When the energy contributions are added, we have the formation energy, enthalpy, Gibbs free energy, and bonding energy (relative to spin-restricted average-of-configuration atomic fragments) at the B3LYP level (Table 2). The formation energy with CCSD(T) single-point calculations is also displayed here to verify the ground states. Except for PuF_8 and $PuOF_6$, which arguably have no chance to form oxidation states lower than VIII (A and B in Figure 1), the other PuO_nF_{8-2n} ($n > 1$) species all prefer the V oxidation state (D, F, and H in Figure 1), in which two oxygen atoms connect with each other to form a superoxide ligand. In order to further check which state could be the most probable product in the same reaction under the conditions of Pu + $2O_2$ + $4F_2$, we selected PuO_2F_4 $^5C_{2v}$ (D) as the relative energy 0 to compare with others. PuO_2F_4 in the $^5C_{2v}$ state has the lowest formation energy over the whole PuO_nF_{8-2n} series.

We divided vibration frequencies according to the vibration mode in Table 3. The Pu−F stretching, Pu−O stretching, and O−O stretching species are in the range of 400−1000 cm^{-1} that could be detected in an experiment. The values of the Pu−F stretching mode are about 400−700 cm^{-1}, the Pu−O stretching mode values are more than 780 cm^{-1}, and the O−O stretching values equal about 1200 cm^{-1}, an increase in the vibration species indicating a bond strength increase. There are no imaginary frequencies for the presented states of PuO_nF_{8-2n}, which means that the states are local minima or ground states.

Table 2. Formation Energy, Enthalpy, Gibbs Free Energy, and Bonding Energy (kcal/mol)[a]

		B3LYP				
species	system	$\Delta(\Delta_f E)$	$\Delta(\Delta_f H)$	$\Delta(\Delta_f G)$	ΔBE	CCSD(T) $\Delta(\Delta_f E)$
A	PuF_8 ^1O_h	−2.84	−1.47	15.18	35.43	25.32
B	$PuOF_6$ $^1C_{2v}$	22.05	22.75	31.52	15.87	23.46
C	PuO_2F_4 $^1D_{4h}$	49.93	50.18	54.21	35.43	40.54
D	PuO_2F_4 $^5C_{2v}$	0.00	0.00	0.00	0.00	0.00
E	PuO_3F_2 ^1C_s	136.56	136.24	133.99	110.53	100.56
F	PuO_3F_2 $^5C_{2v}$	105.96	105.28	101.29	97.66	97.23
G	PuO_4 $^1D_{4h}$	219.33	218.12	213.45	187.23	177.66
H	PuO_4 $^5C_{2v}$	194.58	193.88	185.90	173.26	171.60

[a] Species D was chosen as 0 to show a clear relative energy among the states.

Table 3. Normal Mode Vibration Frequencies (cm^{-1}) of the PuO_nF_{8-2n} Isomers at the B3LYP Level

species	system, symmetry	Pu−F[a]	Pu−O[a]	O−O[a]	$Pu<O_2$	FPuF[a]	OPuF[b]	OPuO[b]
A	PuF_8 ^1O_h	A_{1g}: 594 T_{1u}: 574 T_{2g}: 460 A_{2u}: 430 E_g: 414				E_u: 68 T_{2g}: 276 T_{1u}: 304 T_{2u}: 381		
B	$PuOF_6$ $^1C_{2v}$	A_1: 612 B_1: 573 B_2: 571 A_2: 494 B_2: 480 A_1: 393	A_1: 842 A_1: 507			A_2: 67 B_1: 214 A_1: 216 A_1: 280 A_2: 293	B_2: 60 B_2: 256 B_1: 311 B_2: 312 B_1: 378	
C	PuO_2F_4 $^1D_{4h}$	E_u: 582 A_{1g}: 563 B_{1g}: 504	A_{2u}: 1006 A_{1g}: 872			B_{2u}: 163 B_{2g}: 196 A_{2u}: 216	E_u: 141 E_g: 233	E_u: 279
D	PuO_2F_4 $^5C_{2v}$	B_2: 703 A_1: 701 B_1: 580 A_1: 528		A_1: 1113	B_2: 446 A_1: 207	A_1: 75 B_2: 111 A_2: 132 A_1: 150	B_2: 67 B_1: 84 B_1: 166	A_2: 271
E	PuO_3F_2 ^1C_s	A′: 567 A′: 533	A″: 959 A′: 864 A′: 784				A′: 122 A′: 167 A″: 180 A″: 252 A′: 267 A″: 283	A′: 316
F	PuO_3F_2 $^5C_{2v}$	B_2: 538 A_1: 527	A_1: 782	A_1: 1222	A_1: 325 B_1: 343	A_1: 177	B_1: 77 B_2: 134 B_1: 139 B_2: 259	A_2: 163
G	PuO_4 $^1D_{4h}$		E_u: 916 A_{1g}: 867 B_{1g}: 728					A_{2u}: 272 E_u: 356 B_{2g}: 378
H	PuO_4 $^5C_{2v}$		B_1: 931 A_1: 841	A_1: 1210	B_2: 392 A_1: 389			B_1: 192 A_2: 204 B_2: 243 A_1: 269

[a] Stretching. [b] Bending.

3.2. Charge Analysis and Electronic Structure of PuO_nF_{8-2n} (n = 0−4) Species.

Not only can the bond length illustrate the oxidation state of Pu but also the effective charge analysis in Table 4 can shed much light on it by the relevant charge value and spin population value. The spins of Pu of D, F, and H states are about 3.5, which suggests three to four single electrons on the plutonium atom. The net charge value on the long-bond oxygen atom equals about one-fourth of the short-bond value. There is little spin population on fluorine and short-bond oxygen; on the other hand, the long-bond oxygen always has about 0.5 spin population. All of the tests show that plutonium has oxidation state V in the open-shell ground state of PuO_2F_4, PuO_3F_2, and PuO_4.

All of the VIII Pu oxidation state geometries are closed shell, while there are three single electrons on Pu and one single electron on O_2^- for Pu(V) geometries. The electronic structures of species D, F, and H are very similar because they all have a V oxidation state Pu that connects with one

Table 4. Calculated Effective Charges of PuO_nF_{8-2n} Isomers

					Mulliken		MDC-q[a]	
species	system, symmetry	atom	Hirshfeld charge	Voronoi charge	charge	spin population	charge	spin population
A	PuF_8 ^1O_h	Pu	1.19	0.94	2.97	0	8.91	0
		F	−0.15	−0.12	−0.37	0	−1.11	0
B	$PuOF_6$ $^1C_{2v}$	Pu	1.17	0.91	2.92	0	4.44	0
		F	−0.18	−0.14	−0.42	0	−0.63	0
		O	−0.10	−0.08	−0.39	0	−0.68	0
C	PuO_2F_4 $^1D_{4h}$	Pu	1.18	−0.91	2.81	0	6.04	0
		F	−0.21	−0.15	−0.47	0	−0.97	0
		O	−0.18	−0.15	−0.47	0	−1.08	0
D	PuO_2F_4 $^5C_{2v}$	Pu	1.11	0.69	2.47	3.52	1.23	−3.65
		F	−0.25	−0.17	−0.54	−0.05	−0.27	0.08
		O (O_2^-)	−0.05	0.00	−0.16	−0.65	−0.08	0.64
E	PuO_3F_2 ^1C_s	Pu	1.18	0.91	2.56	0	1.66	0
		F	−0.26	−0.20	−0.54	0	−0.40	0
		O	−0.22	−0.17	−0.50	0	−0.29	0
F	PuO_3F_2 $^5C_{2v}$	Pu	1.14	0.81	2.09	3.58	1.96	−3.70
		F	−0.33	−0.25	−0.57	−0.02	−0.50	0.06
		O	−0.32	−0.27	−0.58	−0.35	−0.50	0.38
		O (O_2^-)	−0.08	−0.02	−0.19	−0.59	−0.22	0.60
G	PuO_4 $^1D_{4h}$	Pu	1.19	0.92	2.16	0	1.64	0
		O	−0.30	−0.23	−0.54	0	−0.41	0
H	PuO_4 $^5C_{2v}$	Pu	1.07	0.85	1.76	3.37	1.64	−3.39
		O	−0.40	−0.33	−0.63	−0.17	−0.54	0.18
		O (O_2^-)	−0.14	−0.09	−0.25	0.48	−0.28	−0.48

[a] Multipole derived charges with quadrupole terms.

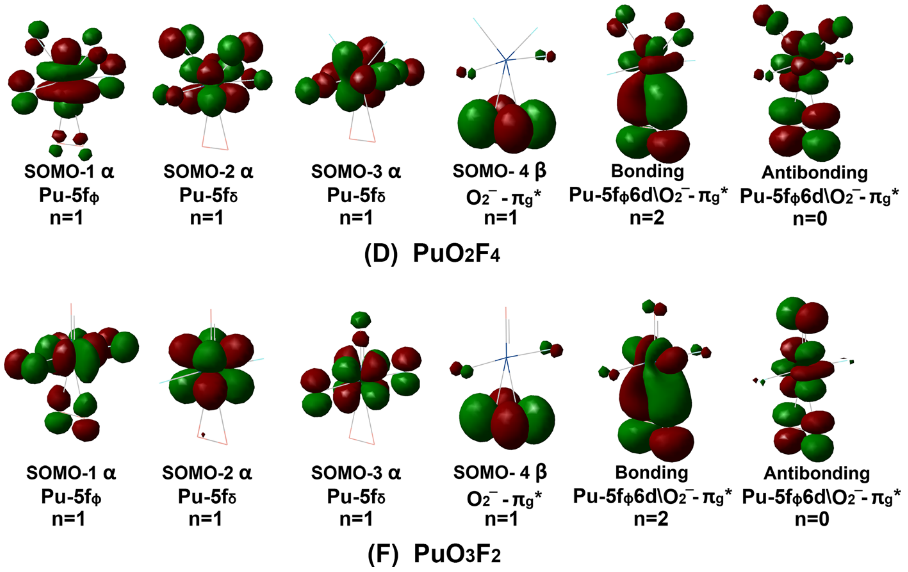

Figure 2. Electronic structures of SOMO and bonding−antibonding B3LYP orbital between O_2^- and Pu for PuO_2F_4 and PuO_3F_2. n is the occupation number.

superoxide. The electronic structures of the SOMO of PuO_2F_4 and PuO_3F_2 are shown in Figure 2, and that of PuO_4 is presented in the work of Huang et al.[9] Even though there are four single electrons in all for the D, F, and H states, that on O_2^- prefers to occupy a β orbital because of spin-polarization effects. The other three unpaired electrons are kept on Pu: two $5f_\delta$ and one $5f_\phi$. The triplet states are 4.61 kcal/mol lower than the quintet states for PuO_2F_4, 3.88 kcal/mol for PuO_3F_2, and 3.35 kcal/mol for PuO_4 at the B3LYP level. The bonding between Pu and the superoxides occurs between a $5f_\phi$ orbital of Pu and π_g* of O_2^-. There is also 5% of a 6d orbital mixed into the bonding. Here we focus on the high-spin states (quintet) because the triplet states share the same electron configuration, although with different spin coupling.

3.3. Reductive Elimination of PuF_8 and $PuOF_6$.

As we mentioned above, PuF_8 and $PuOF_6$ could have isomers of oxidation state VIII if reactions are not considered. Both of them may undergo a reductive elimination and decompose to $Pu^{VI}F_6$ with a ΔE value as high as −90 kcal/mol. For the potential barrier of PuF_8, the F−F bond in F_2 is much softer than the O−O bond in O_2. Therefore, we present the reductive elimination process of eq 2 in Figure 3. PuF_6 was optimized at

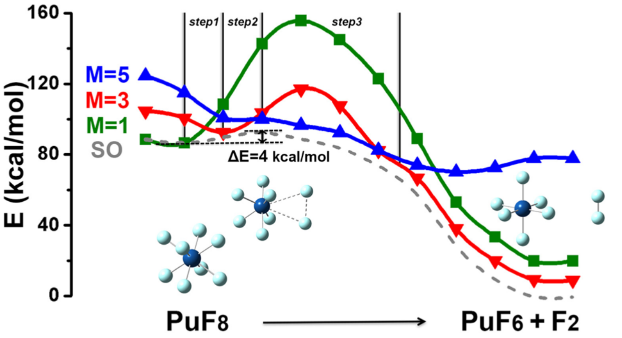

Figure 3. Linear transition curve from PuF_8 (O_h) to PuF_6 (O_h) + F_2 for the spin multiplicities M = 1, 3, 5, at the B3LYP level. The M = 1−5 quasi-relativistic curves use LS quantization. The lowest, dashed curve includes SO coupling.

the B3LYP leve,l and the Pu−F bond length is 1.99 Å in O_h symmetry. The electronic state was kept as $f^2\ {}^3T_{1g}$, with one $t_{2u}(f_\delta/f_\phi)$ and one $a_{2u}(f_\delta/f_\phi)$ electron. Spin−orbit coupling effects lead to a 4 kcal/mol reduction, causing eq 2 being more exothermic. The active space of CASSCF/CASPT2/SO calculations was chosen as shown in Figure S2 in the Supporting Information.

$$PuF_8 \xrightarrow{\Delta_f E_1} PuF_6 + F_2$$

$$\Delta_f E_1 \mathrm{CCSD}(T) = -90.52\ \mathrm{kcal/mol} \quad (2)$$

$$PuOF_6 \xrightarrow{\Delta_f E_2} PuF_6 + 1/2O_2$$

$$\Delta_f E_2 \mathrm{ccsd}(t) = -88.65\ \mathrm{kcal/mol} \quad (3)$$

According to the reaction rate of formula 4,[59] the barrier E_a from PuF_8 to PuF_6 + F_2 is about 17 kcal/mol (Figure 3). The zero-point energy plays an important role in the reaction potential and reduces the potential energy barrier to 13 kcal/mol. The spin−orbit interaction gives a further reduction of 9 kcal/mol, leaving a final dissociation barrier of 4 kcal/mol. As a result, one can obtain the reaction rate $v = 1.16 \times 10^{10}\ s^{-1}$ at 298 K, with the frequency $v_0 = 1 \times 10^{13}\ s^{-1}$, a reasonable value suggested in a study by Marrochelli and Wang in their Supporting Information files.[60,61] With the reaction rate 10^{10} s^{-1}, the PuF_8 molecule would instantaneously decompose (see Figure 3). What is more, this small estimated decomposition barrier might be even smaller or even not exist in the real situation. The active orbitals and occupation number in CASSCF/CASPT2/SO calculation of the barrier point are shown in Figure S3 in the Supporting Information.

$$v = v_0 \exp(-E_a/k_B T) \quad (4)$$

We included as a model for solvation a COSMO model of H_2O solvation. It contributes 2.16 kcal/mol reduced energy for $\Delta_f E_1$ and 2.29 kcal/mol for $\Delta_f E_2$ at the B3LYP level, suggesting that both PuF_8 and $PuOF_6$ are reduced more easily in the solution phase than in the gas phase. Indeed, the highest oxidation state Pu(VIII) can hardly survive under solvation conditions, because such a species is so strong an oxidizing agent that the possibility of oxidizing the solvent cannot be excluded.

We separate the reductive elimination process of the Pu(VIII) species in three steps according to the electron transfer, as shown in Figure 4. In step 1, after removal of two fluorine atoms, one electron first goes back to plutonium to form Pu(VII), and the second isomer has two single electrons, one on the 5f orbital of Pu(VII) and one shared between the 2p orbitals of the two leaving F atoms. In step 2, the two fluorines are further out, and the other electron jumps back to plutonium to form Pu(VI). As a consequence, the third isomer has four single electrons, two on the 5f orbital of plutonium and two electrons on the two leaving F atoms. Now, the plutonium atom is already hexavalent. In step 3, finally, the two leaving F atoms attract each other and form an F_2 molecule. The PuF_6 part has two single electrons on Pu(VI) and finally settles on an O_h symmetry. The strong exothermicity of $PuF_8 \rightarrow PuF_6 + F_2$ and low energy barrier are consistent with the experimental evidence that PuF_6 exists while PuF_8 has been undetected so far.

3.4. Other Possible $Pu^{VIII}O_2F_5^-$ Anions. As actinyls often prefer an equatorial pentacoordination, we also tested the possibility of a $PuO_2F_5^-$ anion in a ${}^1D_{5h}$ state as a potential Pu(VIII) species. The point of comparison was again a peroxide species, with a ${}^5C_{2v}$ structure (see Figure 5). The four unpaired electrons of the latter were the three ($2f_\delta\ 1f_\phi$) on Pu and the the single π^* electron on O_2^-. Of them, the latter open-shell Pu(V) species was found to lie lower, by 82 and 88 kcal/mol at the B3LYP and CCSD(T) levels, respectively.

3.5. Parallel Case: Fe(VIII) and FeO_4. The direct observation of iron tetroxide, FeO_4,[62] has not been confirmed by any other group. Some comfort is given here by the photoelectron spectra neutralizing FeO_4^- to FeO_4 by Wang's group.[63] A theoretical treatment also exists.[64] Remarkably, Tran and Hendrix[64] found that the experimental PES is a

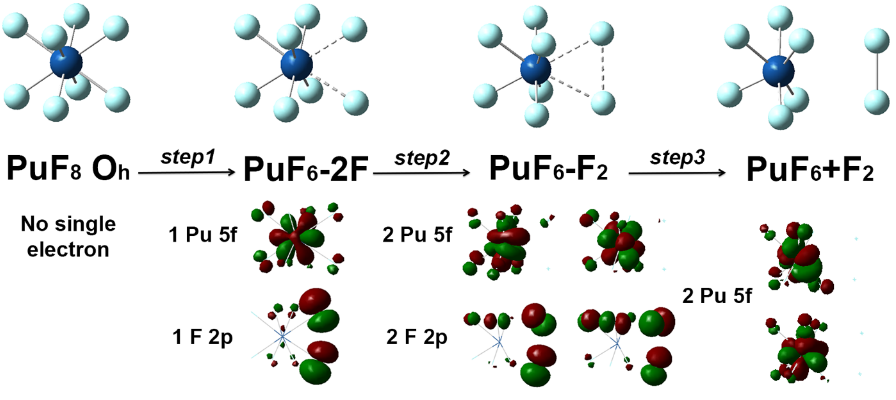

Figure 4. Electron transfer process for PuF_8 reductive elimination to PuF_6 and F_2 and the electronic structure of the intermediates.

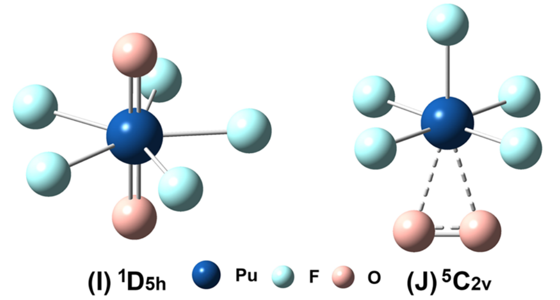

Figure 5. Structures of the anion $PuO_2F_5^-$: (I) $^1D_{5h}$ state with Pu(VIII) (a local minimum); (J) $^5C_{2v}$ state with Pu(V) (the absolute minimum)).

superposition of both oxidation states Fe(VIII) and Fe(VI). Similar calculations using the same CASPT2 methods used by us confirm the theoretical result that the structure $Fe^{VI}O_2O_2$ ($^1C_{2v}$) is 5.8 kcal/mol above the structure $Fe^{VIII}O_4$ (^1T_d). Here we tentatively represent FeO_4 (^1T_d) as having Fe(VIII) oxidation state, which is a controversial issue that needs to be discussed in the future. As approximately calculated in ref 9, the structures $Pu^{VIII}O_4$ (D_{4h}) and $Pu^VO_2O_2$ (C_{2v}) are separated by a relatively high barrier and could therefore coexist. Such cases are PuO_3F_2, PuO_2F_4, and $PuO_2F_5^-$ anion. Figures S4–S6 in the Supporting Information separately present the linear transition curve with a high barrier. Note that these barriers are approximately calculated only for the purpose of estimation and their accurate calculation including sophisticated electron correlation and spin–orbit coupling effects are too expensive to be done at present.

3.6. New Experimental Suggestions. None of the species studied here are calculated to have a Pu(VIII) ground state. Therefore, even accepting at face value the thermochromatographic[26] and liquid-state extraction[27] observations, it would appear premature, if not sanguine, to draw the conclusion of Pu(VIII) chemistry. One possibility is that such species of unknown disintegration lifetime have indeed been present.

At a frankly speculative level one could suggest an experiment where one would irradiate a compound such as $M_3[UO_2F_5]$ (M = Na–Cs), in a nuclear reactor.[3] Then the nuclear reaction

$$^{238}_{92}\mathrm{U} \xrightarrow{+n} {}^{239}_{92}\mathrm{U} \xrightarrow{-\beta} {}^{239}_{93}\mathrm{Np} \xrightarrow{-\beta} {}^{239}_{94}\mathrm{Pu} \tag{5}$$

could directly create the present $PuO_2F_5^-$ anion. A subsequent laser ablation time-of-flight mass separation plus photoelectron spectroscopy could possibly provide more detailed evidence of the system at hand, even with minute amounts of $^{239}_{94}Pu$. The possibilities are given in Table 5.

4. CONCLUSIONS

After considering the geometry, electronic structure, and bonding analysis of the PuF_nO_{8-2n} (n = 0–4) species, we find no Pu(VIII) isomers that are global minima. Instead, reductive elimination reactions of the Pu(VIII) species to produce O_2 or F_2 may occur. In certain cases, however, the barrier for these reactions can be broad and high, and hence the kinetically metastable species could perhaps coexist, especially as a transient species in the gas phase. An interesting precedent where this situation seems to have been experimentally observed is $Fe^{VIII}O_4$; such Pu(VIII) cases are PuO_4, PuO_3F_2, PuO_2F_4, and the $PuO_2F_5^-$ anion. The cases PuF_8 and $PuOF_6$ do not have sufficient barriers to sustain a Pu(VIII) oxidation state. Examples of hypothetical nuclear reactions leading to Pu(VIII) species are presented.

Table 5. Experimental Suggestions for Pu(VIII)

reactant	product
$[UO_2F_5]^{3-}$	$[PuO_2F_5]^-$
$[UO_4]^{2-}$	$[PuO_4]$
$[UF_8]^{2-}$	$[PuF_8]$

■ ASSOCIATED CONTENT

Ⓢ Supporting Information

The Supporting Information is available free of charge on the ACS Publications website at DOI: 10.1021/acs.inorgchem.5b01540.

Full references to the software used in this study and additional structural and computational data (PDF)

■ AUTHOR INFORMATION

Corresponding Authors

*E-mail for P.P.: Pekka.Pyykko@helsinki.fi.
*E-mail for J.L.: junli@tsinghua.edu.cn.

Notes

The authors declare no competing financial interest.

■ ACKNOWLEDGMENTS

P.P. thanks the Magnus Ehrnrooth Foundation for travel scholarships in 2015. This work was financially supported by the NKBRSF (Grant No. 2013CB834603) and NSFC (Grant Nos. 91426302, 21433005, and 21201106) of China and was performed using supercomputers at Tsinghua National Laboratory for Information Science and Technology and the Supercomputing Center, Computer Network Information Center of the Chinese Academy of Sciences.

■ REFERENCES

(1) Karen, P.; McArdle, P.; Takats, J. *Pure Appl. Chem.* **2014**, *86*, 1017–1081.

(2) Ionova, G. V.; Mironov, V. S.; Spitsyn, V. I.; Pershina, V. G. *Soviet Radiochem.* **1981**, *23*, 1–5.

(3) Straka, M.; Dyall, K. G.; Pyykkö, P. *Theor. Chem. Acc.* **2001**, *106*, 393–403.

(4) Nikonov, M.; Gogolev, A.; Tananaev, I.; Myasoedov, B. *Radiochemistry* **2004**, *46*, 340–342.

(5) Tananaev, I. G.; Nikonov, M. V.; Myasoedov, B. F.; Clark, D. L. *J. Alloys Compd.* **2007**, *444-445*, 668–672.

(6) Kiselev, Yu. M.; Nikonov, M. V.; Tananaev, I. G.; Myasoedov, B. F. *Dokl. Phys. Chem.* **2009**, *425*, 73–76.

(7) Nikonov, M. V.; Myasoedov, B. F. *Radiochemistry* **2010**, *52*, 17–21.

(8) Antonio, M. R.; Williams, C. W.; Sullivan, J. A.; Skanthakumar, S.; Hu, Y.-J.; Soderholm, L. *Inorg. Chem.* **2012**, *51*, 5274–5281.

(9) Huang, W.; Xu, W.-H.; Su, J.; Schwarz, W. H. E.; Li, J. *Inorg. Chem.* **2013**, *52*, 14237–14245.

(10) Zaitsevskii, A. V.; Titov, A. V.; Malkov, S. S.; Tananaev, I. G.; Kiselev, Y. M. *Dokl. Chem.* **2013**, *448*, 1–3.

(11) Zaitsevskii, A. V.; Mosyagin, N. S.; Titov, A. V.; Kiselev, Y. M. *J. Chem. Phys.* **2013**, *139*, 034307.

(12) Wells, A. F. *Structural Inorganic Chemistry*, 5th ed.; Oxford University Press: Oxford, U.K., 1984.

(13) Riedel, S.; Kaupp, M. *Coord. Chem. Rev.* **2009**, *253*, 606–624.

(14) Himmel, D.; Knapp, C.; Patzschke, M.; Riedel, S. *ChemPhysChem* **2010**, *11*, 865−869.
(15) Rother, P.; Wagner, F.; Zahn, U. *Radiochim. Acta* **1969**, *11*, 203−210.
(16) Wang, G.; Zhou, M.; Goettel, J. T.; Schrobilgen, G. J.; Su, J.; Li, J. *Nature* **2014**, *514*, 475−477.
(17) Pyykkö, P.; Xu, W.-H. *Chem. - Eur. J.* **2015**, *21*, 9468−9473.
(18) Hu, H.-S.; Wei, F.; Wang, X.; Andrews, L.; Li, J. *J. Am. Chem. Soc.* **2014**, *136*, 1427−1437.
(19) Jiang, N.; Schwarz, W. H. E.; Li, J. *Inorg. Chem.* **2015**, *54*, 7171−7180.
(20) Cao, G.-J.; Schwarz, W. H. E.; Li, J. *Inorg. Chem.* **2015**, *54*, 3695−3701.
(21) Su, J.; Hu, S.-X.; Huang, W.; Zhou, M.-F.; Li, J. *Sci. China Chem.* **2015**, DOI: 10.1007/s11426-015-5481-z.
(22) Malm, J. G.; Weinstock, B.; Claassen, H. H. *J. Chem. Phys.* **1955**, *23*, 2192−2193.
(23) Wadt, W. R. *J. Chem. Phys.* **1987**, *86*, 339−346.
(24) Hay, P. J.; Martin, R. L. *J. Chem. Phys.* **1998**, *109*, 3875−3881.
(25) Neidig, M. L.; Clark, D. L.; Martin, R. L. *Coord. Chem. Rev.* **2013**, *257*, 394−406.
(26) Domanov, V. P.; Buklanov, G. V.; Lobanov, Yu. V. *J. Nucl. Sci. Technol.* **2002**, *39*, 579−584.
(27) Kiselev, Yu. M.; Nikonov, M. V.; Dolzhenko, V. D.; Ermilov, A. Yu.; Tamanaev, I. G.; Myasoedov, B. F. *Radiochim. Acta* **2014**, *102*, 227−237.
(28) Zaitsevskii, A.; Schwarz, W. H. E. *Phys. Chem. Chem. Phys.* **2014**, *16*, 8997−9001.
(29) Kubatko, K.-A. H.; Helean, K. B.; Navrotsky, A.; Burns, P. C. *Science* **2003**, *302*, 1191−1193.
(30) Unruh, D. K.; Burtner, A.; Pressprich, L.; Sigmon, G. E.; Burns, P. C. *Dalton Trans.* **2010**, *39*, 5807−5813.
(31) Pyykkö, P.; Zhao, Y. *J. Phys. Chem.* **1990**, *94*, 7753−7759.
(32) Dua, S.; Bowie, J. H. *J. Phys. Chem. A* **2003**, *107*, 76−82.
(33) O'Grady, E.; Kaltsoyannis, N. *Dalton Trans.* **2002**, *2002*, 1233−1239.
(34) Pyykkö, P.; Runeberg, N.; Straka, M.; Dyall, K. G. *Chem. Phys. Lett.* **2000**, *328*, 415−419.
(35) Xiao, H.; Hu, H.-S.; Schwarz, W. H. E.; Li, J. *J. Phys. Chem. A* **2010**, *114*, 8837−8844.
(36) Pyykkö, P. *Phys. Chem. Chem. Phys.* **2011**, *13*, 161−168.
(37) Frisch, M., et al. *Gaussian*; Gaussian, Wallingford, CT, 2010.
(38) Baerends, E. J., et al. *ADF*; SCM, Vrije Universiteit, Amsterdam, 2013.
(39) Werner H.-J., et al. *MOLPRO*; www.molpro.net, 2012.
(40) Becke, A. D. *J. Chem. Phys.* **1993**, *98*, 5648−5652.
(41) Küchle, W.; Dolg, M.; Stoll, H.; Preuss, H. *J. Chem. Phys.* **1994**, *100*, 7535−7542.
(42) Cao, X.-Y.; Dolg, M.; Stoll, H. *J. Chem. Phys.* **2003**, *118*, 487−496.
(43) Cao, X.-Y.; Dolg, M. *J. Mol. Struct.: THEOCHEM* **2004**, *673*, 203−209.
(44) Kendall, R. A.; Dunning, T. H.; Harrison, R. J. *J. Chem. Phys.* **1992**, *96*, 6796−6806.
(45) Raghavachari, K.; Trucks, G. W.; Pople, J. A.; Head- Gordon, M. *Chem. Phys. Lett.* **1989**, *157*, 479−483.
(46) Watts, J. D.; Gauss, J.; Bartlett, R. J. *J. Chem. Phys.* **1993**, *98*, 8718−8733.
(47) Knowles, P. J.; Hampel, C.; Werner, H.-J. *J. Chem. Phys.* **1993**, *99*, 5219−5227.
(48) Bartlett, R. J.; Musiał, M. *Rev. Mod. Phys.* **2007**, *79*, 291−352.
(49) Schmidt, M. W.; Gordon, M. S. *Annu. Rev. Phys. Chem.* **1998**, *49*, 233−266.
(50) Celani, P.; Werner, H.-J. *J. Chem. Phys.* **2000**, *112*, 5546−5557.
(51) Shiozaki, T.; Gyorffy, W.; Celani, P.; Werner, H.-J. *J. Chem. Phys.* **2011**, *135*, 081106.
(52) Berning, A.; Schweizer, M.; Werner, H.-J.; Knowles, P. J.; Palmieri, P. *Mol. Phys.* **2000**, *98*, 1823−1833.
(53) van Lenthe, E.; Baerends, E. J.; Snijders, J. G. *J. Chem. Phys.* **1993**, *99*, 4597−4610.
(54) Perdew, J. P.; Burke, K.; Ernzerhof, M. *Phys. Rev. Lett.* **1996**, *77*, 3865−3868.
(55) van Lenthe, E.; Baerends, E. J. *J. Comput. Chem.* **2003**, *24*, 1142−1156.
(56) Baerends, E. J.; Ellis, D. E.; Ros, P. *Chem. Phys.* **1973**, *2*, 41−51.
(57) Andrews, L. *J. Phys. Chem.* **1969**, *73*, 3922−3928.
(58) Straka, M.; Patzschke, M.; Pyykkö, P. *Theor. Chem. Acc.* **2003**, *109*, 332−340.
(59) Dushman, S. *J. Am. Chem. Soc.* **1921**, *43*, 397−433.
(60) Marrocchelli, D.; Yildiz, B. *J. Phys. Chem. C* **2012**, *116*, 2411−2424.
(61) Wang, Y.-G.; Mei, D.; Li, J.; Rousseau, R. *J. Phys. Chem. C* **2013**, *117*, 23082−23089.
(62) Kiselev, Y. M.; Kopelev, N. S.; Bobylev, A. P. *Russ. J. Inorg. Chem.* **1989**, *34*, 2654.
(63) Wu, H.; Desai, S. R.; Wang, L.-S. *J. Am. Chem. Soc.* **1996**, *118*, 5296−5301.
(64) Tran, V. T.; Hendrickx, M. F. A. *J. Chem. Phys.* **2011**, *135*, 094505.